QUANTITATIVE ANALYSIS OF AL INFLOUR PRODUCTS BY LASER-INDUCED BREAKDOWN SPECTROSCOPY COMBINED WITH PARTIAL LEAST SQUARES

Q. Ding*, M. Yao, Sh. Wu, M. Zeng, N. Xue, D. Wu, J. Xu*

College of Engineering at Jiangxi Agricultural University, Nanchang, China;
e-mail: dqp0022@163.com, xujiangstart@163.com

Based on partial least squares (PLS) analysis, the effects of different smoothing points and different preprocessing methods on the accuracy and precision of the PLS model were compared and analyzed. The results show that the PLS quantitative model has the best effect when using 11-point smoothing combined with standard normal variables (SNVs) as the preprocessing method. The coefficients of determination (R_c^2, R_p^2) of the model training set and prediction set are 0.9900 and 0.9996, respectively. The root means square errors (RMSECV, RMSEP) are 11.7 and 5.23, respectively, and the average relative error of prediction is only 2.96%, which indicates a high prediction accuracy rate and accuracy. This work demonstrates that LIBS technology has broad application prospects for the quantitative detection of specific ingredients in flour products and provides a basis for the real-time monitoring and evaluation of food safety.

Keywords: *Laser-induced breakdown spectroscopy, flour products, quantitative analysis, aluminum element, partial least squares.*

ОПРЕДЕЛЕНИЕ СОДЕРЖАНИЯ АЛЮМИНИЯ В МУЧНЫХ ИЗДЕЛИЯХ МЕТОДОМ ЛАЗЕРНОЙ АТОМНО-ЭМИССИОННОЙ СПЕКТРОСКОПИИ В СОЧЕТАНИИ С МЕТОДОМ НАИМЕНЬШИХ КВАДРАТОВ

Q. Ding*, M. Yao, Sh. Wu, M. Zeng, N. Xue, D. Wu, J. Xu*

УДК 543.423:546.621/.623

Инженерный колледж Сельскохозяйственного университета Цзянси, Наньчан, Китай; e-mail: dqp0022@163.com, xujiangstart@163.com

(Поступила 20 сентября 2021)

С использованием метода наименьших квадратов (PLS) проведены сравнение и анализ влияния различных точек сглаживания и различных методов предварительной обработки на точность модели PLS. Показано, что количественная модель PLS дает наилучший эффект при использовании 11-точечного сглаживания в сочетании со стандартными нормальными переменными (SNVs) в качестве метода предварительной обработки. Коэффициенты детерминации R_c^2 и R_p^2 обучающего набора модели и набора прогнозирования составляют 0.9900 и 0.9996. Среднеквадратичные ошибки RMSECV = 11.7 и RMSEP = 5.23, средняя относительная ошибка прогнозирования 2.96% указывает на высокий уровень точности и точности прогнозирования. Продемонстрированы перспективы применения лазерной атомно-эмиссионной спектроскопии для количественного определения конкретных ингредиентов в мучных изделиях в качестве основы для мониторинга и оценки безопасности пищевых продуктов в режиме реального времени.

Ключевые слова: *лазерная атомно-эмиссионная спектроскопия, мучные изделия, количественный анализ, алюминиевый элемент, метод наименьших квадратов.*

Introduction. Flour products are one of the most common and popular ready-to-eat foods in China [1–3]. Owing to the influence of traditional eating habits, flour products occupy an important position in the diet of Chinese residents and are an important carrier for the human body to take in trace elements such as

iron, calcium, zinc, folic acid, vitamin A, and vitamin B1 [4, 5]. Alum, namely aluminum sulfate or aluminum potassium sulfate, is commonly used as a raising agent for flour products [6, 7]. In the production process of flour products, some unscrupulous vendors add a relatively large amount of alum, which causes serious harm to human health in the daily diet, to give the food made with flour a crisp and porous texture.

Studies in recent years have shown that aluminum is not an essential element for the human body but a low-toxic element. The nervous system is one of the main target organs of aluminum. Excess aluminum can interfere with the consciousness and memory function of the human brain. This will cause the human body to have visual movement coordination failure and long-term memory loss. In severe cases, patients will suffer from diseases such as Alzheimer's and Parkinson's [8, 9]. The Food and Agriculture Organization/World Health Organization (FAO/WHO) recommends a provisional tolerable weekly intake (PTWI) of 2 mg/kg (bodyweight; 2011), and the National Standard of China (GB2760-2014) clearly states that the Al remaining in flour products should be less than 100 mg/kg (per dry mass of food) [6, 10, 11]. Therefore, high concentrations of aluminum in flour products are associated with adverse health effects, and the fast and accurate detection of aluminum pollution in flour products is urgently needed to ensure food safety, improve the food production environment, and reduce the risk of Al poisoning [12].

At present, the methods for determining aluminum content in food mainly include spectrophotometry, atomic absorption spectrometry (AAS) [13], inductively coupled plasma emission spectrometry (ICP-OES) [14], and inductively coupled plasma–mass spectrometry (ICP-MS) [15]. However, the current food analysis technology has disadvantages such as long detection time, high cost, and difficulty in setting up systems for on-site detection. For example, the use of spectrophotometry to detect aluminum content requires the preparation of multiple chemical reagents, has a cumbersome detection process, and a large workload. The ICP-OES and AAS methods are prone to generate a large amount of toxic waste and require expensive reagents, fume hoods, and sample dissolution; thus, sample preparation is very laborious. The ICP-MS method is expensive and cannot be widely used. Therefore, the traditional detection technology of aluminum-containing additives has obvious limitations. These shortcomings make it difficult to achieve the rapid detection of heavy metals and create systems for real-time monitoring, and may not satisfy the demand for rapid screening analysis at the production site [12, 16].

Laser-induced breakdown spectroscopy (LIBS) has a number of advantages, such as allowing fast or online analysis, allowing the simultaneous measurement of multiple elements, and requiring little to no sample preparation [17]. Currently, LIBS technology has been widely used in an increasing number of scientific studies. Its application fields have also been continuously expanded, such as use in nuclear power plant safety monitoring [18], biomedicine [19], environmental monitoring [20], soil composition monitoring [21], space exploration [22], hazardous explosive monitoring [23], and food safety composition detection [24]. Currently, publications employing the technique for both qualitative and quantitative analysis of elements in various solid food samples can be found throughout the literature [25]. Tian et al. [26] used LIBS combined with the support vector machines (SVMs) method to quickly detect the phosphorus content of three kinds of seafood, cod, scallops, and shrimp, which proved the ability of LIBS combined with machine learning in the determination of phosphorus in seafood products. Therefore, this combination of methods can be used for on-site phosphate detection in the food supply chain. Pervin et al. [27] combined LIBS technology with partial least squares discriminant analysis (PLS-DA) to classify flour samples based on the type of flour and the LIBS spectrum of the mixture and used PLS to determine the ratio of sorghum in the sorghum/maize flour mixture based on the elemental composition. Cama-Moncunill et al. [25] used LIBS combined with multivariate analysis to quantitatively analyze the calcium content of liquid food product samples. This proved the feasibility of the LIBS method to detect calcium in infant formula milk powder, and the detection limit reached 3.69 mg/g. Costa et al. [28] used LIBS to directly determine the content of calcium, potassium, and magnesium in cassava flour samples. Velioglu et al. [29] used LIBS combined with the PCA method to successfully classify the types of internal organs, namely, the beef kidney, liver, heart, lung, and spleen.

A large amount of research data shows that LIBS technology can analyze the content of heavy metals and other elements in food samples in real time, quickly, qualitatively, and quantitatively. The new method is expected to provide both the food industry and governmental agencies with a rapid and simple technique for aluminum quantification in aluminum-containing flour products [30].

In this work, 14 kinds of doughs with different aluminum concentrations were prepared as standard samples. Laser-induced breakdown spectroscopy technology combined with PLS was used to predict the aluminum content in the flour products. Under the same test conditions, spectral data were preprocessed by different preprocessing methods, PLS modeling was performed separately, and the influence of different

preprocessing methods on the quality of the model was analyzed. The results show that the PLS quantitative model has the best effect when using 11-point smoothing combined with SNV as the preprocessing method.

Materials and methods. *LIBS System.* A schematic diagram of the LIBS system used in the research is shown in Fig. 1. A Q-switched Nd:YAG pulsed laser (Beamtech, Vlite-200, China) was used as the ablation source with a laser pulse frequency of 1–10 Hz, a pulse wavelength of 1064 nm, and a laser energy of 0–300 mJ. The laser beam was focused on the surface of the sample through a mirror and a quartz lens with a focal length of 100 mm. The sample was placed on a two-dimensional rotating translation stage (Zolix, SC300-1A, China) to change the analysis position of the sample. The optical fiber probe was used to collect and transmit the plasma emission spectrum to a high-resolution spectrometer (Avantes, AvaSpec-2048FT-8R, Netherlands). The wavelength of the spectrometer was 200–1100 nm. In the experiment, a digital pulse delay generator was used to synchronously control the laser and spectrometer.

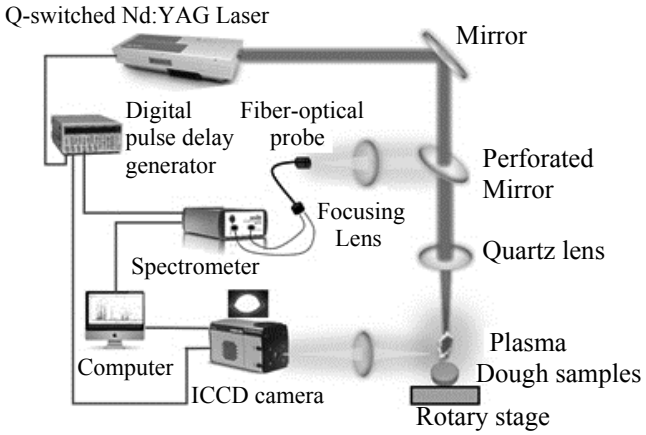

Fig. 1. Schematic diagram of the LIBS system.

Sample preparation. Taking homemade dough as the research object, wet dough was prepared for the experiment containing different concentrations of aluminum potassium sulfate dodecahydrate. The formula for flour food contained 100 g of flour, 1.7 g of salt, varying amounts of aluminum potassium sulfate, and 54 g of deionized water. The amount of aluminum potassium sulfate was determined according to the traditional formula of flour products (data not shown). Food-grade medium-gluten wheat flour was purchased from Jinshahe Flour Group (Hebei, China). Alum ($KAl(SO_4)_2 \cdot 12H_2O$, AR, ≥99.5%) was purchased from Macleans Biochemical Technology (Shanghai, China). In the experiment, the doped samples were vortexed and stirred by a fully automatic kneading machine (HMJ-D4; Liven, Beijing, China) for 20 min. The 14 dough samples with different concentration series were prepared with concentrations of 5, 20, 40, 60, 80, 100, 120, 150, 180, 200, 220, 250, 275, and 300 mg/kg.

The dough sample was processed into a tablet to reduce the interference of the physical form of the sample on the measurement result. The sample was made into a sheet with a diameter of 30 mm at a pressure of 15 MPa using a PP-20S fully automatic powder tablet press (Jingtuo Instrument Technology, Tianjin, China).

Measurements. In this study, LIBS experimental equipment built by the laboratory was used to collect the spectral data of the samples. To prevent the laser beam from repeatedly hitting the same point on the dough surface, the samples were placed on a two-dimensional rotating translation table. The plasma collection delay time was 1.28 μs, the laser energy was 171.5 mJ, and the integration time of the spectrometer was set to 2 ms. Each spectrum accumulated 10 pulses, and 10 spectra were collected for each tablet.

Results and discussion. With reference to the standard spectral lines of the US NIST database, the main characteristic spectral lines of Al in flour products are Al I 394.400 nm and Al I 396.152 nm. In this study, the 390~398 nm band containing two main characteristic spectral lines was selected for PLS modeling analysis, which slightly improved the results of the coefficient of determination (R^2) and root mean square error (RMSE), especially in cross-validation. Figure 2 shows the typical LIBS spectral data information collected within the wavelength range 394–396.5 nm for six dough samples with Al concentrations.

Six dough samples with different concentrations were randomly selected for the pre-experiment. Under the same test parameters, the LIBS spectra of samples with Al concentrations of 20, 40, 80, 120, 200, and 250 ppm were collected. Figure 2 shows that the two spectral lines of Al I 394.400 nm and Al I 396.152 nm

are smooth and clear, with high sensitivity and high emission intensity. Therefore, the Al I 394.400 nm and Al I 396.152 nm spectral lines were selected as the analysis characteristic spectrum in this study. The spectral intensity of the two spectral lines increases with increasing Al concentration. The experimental results accurately reflect the presence of Al and the gradient law of spectral line intensity changing with concentration, indicating that it is feasible to perform quantitative analysis of Al in flour products by LIBS.

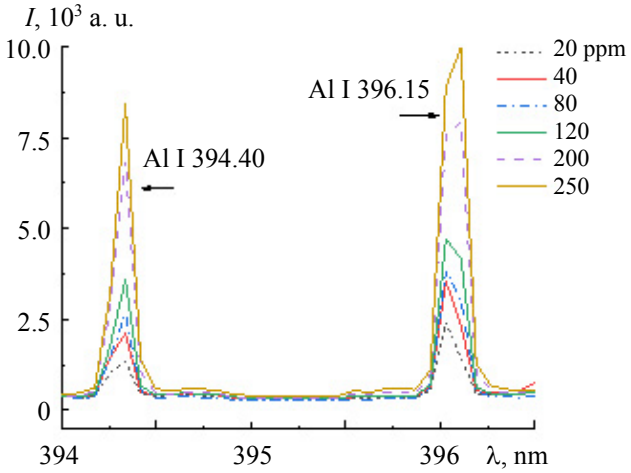

Fig. 2. Typical LIBS spectra of six dough samples with Al concentrations within the 394–396.5 nm range.

Data preprocessing. The LIBS spectrum signal is directly affected mainly by various objective factors, such as the fluctuation of laser particle energy of the laser, the difference in the resolution of the spectrometer, the heterogeneity of the test sample, and the interference of the external environment [31]. To effectively eliminate or attenuate this interference information, the LIBS spectrum data were spectrally preprocessed. With the goal of improving the fit and accuracy of the regression, multivariate analysis with PLS and spectral preprocessing was explored.

First, the LIBS data were preprocessed by spectral smoothing. The smoothing of different points has different effects on the analysis effect of the PLS model. In this paper, the prediction set correlation coefficient (R_p) of the model and the root mean square error of prediction (RMSEP) are used to measure the prediction of the PLS model. R_p is an important indicator to measure the linear correlation between the true concentration of the sample and the predicted concentration. RMSEP was used to measure the prediction accuracy of the model. The value of RMSEP [32] can be calculated using the following equation:

$$\text{RMSEP} = \sqrt{\sum_{i=1}^{n_p} (\hat{y}_{pi} - y_{pi})^2 / n_p} \ .$$

Among them, n_p is the number of samples in the prediction set. y_{pi} and $\hat{y}_{pi}$ are the reference concentration value and the predicted concentration value of the i-th sample respectively. When the R_p value is larger, the RMSEP value is smaller, which means that the prediction accuracy of the model is higher. Table 1 shows the effect of the smoothing of different points on the quality of model prediction. From the table, when the number of smoothing points is 11, the correlation coefficient R_p value reaches 0.9998, and the minimum RMSEP value is 5.23. At this time, the model has the best effect.

TABLE 1. Comparison of Different Point Smoothing Effects on the Quality of the PLS Model

Smoothing points	R_p	RMSEP
0	0.9941	24.6
1	0.9941	24.6
3	0.9435	38.2
5	0.9650	31.1
7	0.9965	10.6
9	0.9983	9.43
11	0.9998	5.23
13	0.9988	5.33

To further eliminate the instability of the quantitative analysis caused by the spectral baseline drift, after the LIBS data were subjected to 11-point smoothing preprocessing, they were sequentially subjected to standard normal variable transformation (SNV), mean centering (MC), first derivative (FD), and second derivative (SD). SNV is a standardized processing method for each spectrum that can eliminate dimensional effects and surface scattering. MC removes the average energy of the data matrix acquired by each instrument. It not only eliminates the influence of index dimension and quantity but also fully reflects the information of the degree of variation and mutual influence of each index in the original data. FD and SD have commonly used baseline correction and spectral resolution preprocessing methods in spectral analysis. Derivation of spectral data can effectively reduce the influence of noise signals. The results of the effects of different spectral preprocessing methods on the quality of the PLS model are shown in Table 2. It can be seen from Table 2 that the four data preprocessing methods can significantly improve the prediction accuracy of the PLS model. After comparative analysis, the R value of the SNV preprocessing method is the largest, and the RMSEP value of the prediction group is the smallest. Compared with the other four preprocessing methods, SNV pretreatment can further improve the accuracy of the PLS model in the quantitative analysis of heavy metal Al content in flour products.

TABLE 2. The Influence of Different Spectral Preprocessing Methods on the Quality of the PLS Model

Pretreatment method	R_p	RMSEP
SNV	0.9998	5.23
Center	0.9991	18.6
FD	0.9986	10.4
SD	0.9988	10.1

PLS model description. The experiment divided 14 samples with concentration gradients into two parts: a training set and a prediction set for modeling. According to the concentration gradient, 1, 4, 7, 10, and 13 were selected as the prediction set samples, and the remaining nine samples were used as the training set samples. According to the spectral information of the Al element in the dough recorded in the experiment, based on the above optimized model parameters, a quantitative correction model for determining the Al content in flour products was established through the PLS chemometric method. The root means square error of cross-validation (RMSECV) and the RMSEP were used to measure the performance of the above quantitative model for Al content detection. R_c^2 and R_p^2 are the determination coefficients of the training set and the prediction set respectively, indicating the accuracy of the calibration model and the prediction model. The experiment used ten principal components (PCs) for modeling. The RMSECV value of the 10 PCs is shown in Fig. 3. When the RMSECV value is the smallest, the corresponding principal component number is 4.

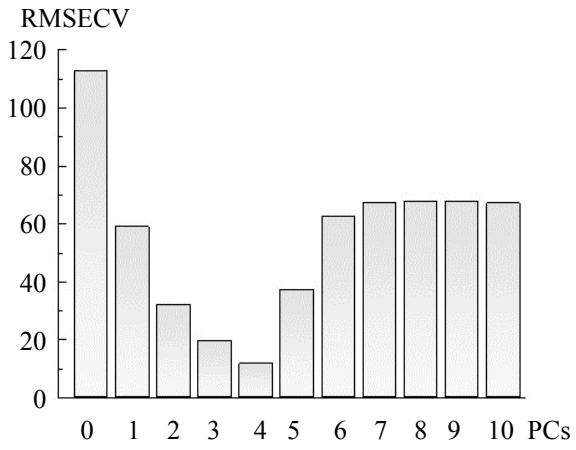

Fig. 3. RMSECV values of PLS models.

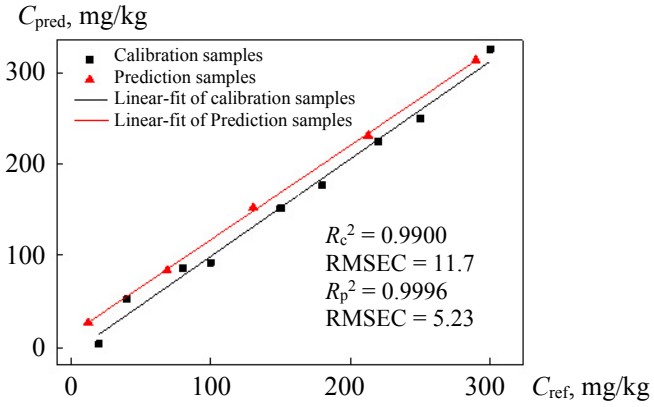

Fig. 4. Quantitative analysis results of the PLS model.

Figure 4 shows the fitting curve of the measured and predicted values of the Al element in the dough samples in the training set and prediction set of the PLS model. It can be seen from the figure that the training set model determination coefficient R_c^2 of the Al element content reaches 0.9900, and RMSECV is 11.7, indicating that the measured value of the Al element in the dough sample of the training set has a good fitting relationship with the predicted value. However, to judge its reliability, the model needs to be verified. The R_p^2 value and RMSEP value of the prediction set result are 0.9996 and 5.23, respectively.

For further analysis of the Al concentration and relative error in the dough samples in the prediction set, see Table 3. It can be clearly seen that the predicted value of the sample is very close to the measured value, and the relative error remains below 6%. Among them, the relative error of two samples is less than 3%, and the average relative error of prediction is 2.96%. The results show that the predicted value of the model and the true value have a good mutual fit. The combination of 11-point smoothing and SNV preprocessing combined with the PLS model has a higher prediction accuracy.

TABLE 3. The Concentration of Al in the Samples of the Prediction Set and the Results of Relative Error Analysis

Sample No.	Reference concentration, mg/kg	Predicted concentration, mg/kg	Absolute error, mg/kg	Relative error, %
1	5	5.1863	0.1863	3.7260
4	60	59.7864	0.2136	0.3560
7	120	126.7614	6.7614	5.6345
10	200	203.4618	3.4618	1.7309
13	275	284.1595	9.1595	3.3072

Conclusions. The experiment prepared 14 dough samples with a concentration gradient of AL element concentrations ranging from 5 to 300 mg/kg. After pressing the dough into a tablet, the spectral information of the 390–398 nm band, including the target Al characteristic spectral lines Al I 394.400 nm and Al I 396.152 nm, was collected and selected. The effects of different smoothing points and different preprocessing methods on the accuracy and precision of PLS modeling were compared and analyzed. Finally, it was concluded that the method of 11-point smoothing combined with SNV preprocessing can effectively reduce the background noise, improve the coefficient of determination (R_c^2, R_p^2) of the calibration model established by PLS and the verification model, and reduce the root mean square error (RMSECV, RMSEP). The R^2 and RMSE of the calibration model and the validation model are 0.9900 and 11.7 and 0.9996 and 5.23, respectively. The average relative error of prediction is only 2.96%. The lowest concentration in the sample group was 5 mg/kg, which was close to the predicted concentration of 5.1863 mg/kg. Therefore, it was preliminarily estimated that the detection limit of quantitative analysis was approximately 5 mg/kg. It can be seen that the quantitative model has good prediction accuracy and sensitivity. The results show that LIBS combined with spectral data processing methods and appropriate stoichiometry methods can reduce the interference of background and noise signals and improve the detection sensitivity and stability of the target heavy metal elements. This technology can be developed into a means and method of quickly supervising food safety and strengthening people's identification and selection of safe food.

Acknowledgments. The authors are grateful to the Jiangxi Province Education Department (No. S202110410073) for financial support.

REFERENCES

1. H. Cao, T. Wang, Y. Min, J. Yu, F. Xu, *J. Food Prot.*, **80**, No. 10, 523–531 (2017).
2. G. Ma, *J. Ethnic Foods*, **2**, No. 4, 195–199 (2015).
3. P. A. Akin, B. Sezer, T. Sanal, H. Apaydin, H. Koksel, İ. H. Boyaci, *J. Cereal Sci.*, **92**, 102920 (2020).
4. F. Liu, C. Zhang, Z. Huang, P. Liu, D. Chen, *J. Instrum. Anal.*, **38**, No. 4, 390–395 (2019).
5. S. Akhtar, F. M. Anjum, M. Akbar Anjum, *Food Res. Int.*, **44**, No. 3, 652–659 (2010).
6. H. Hua, X. Jiang, S. Wu, *Food Chem.*, **207**, 1–5 (2016).
7. A. M. Abdulwahab, Y. A. A. Al-Magdashi, A. Meftah, D. A. Al-Eryani, A. A. Qaid, *Chin. J. Phys.*, **60**, 510–521 (2019).
8. S. Sarin, D. Julka, K. D. Gill, *Mol. Cell. Biochem.*, **168**, 95–100 (1997).
9. J. L. Greger, C. F. Powers, *Toxicology*, **76**, No. 2, 119–132 (1992).
10. R. O. Oruko, J. N. Edokpayi, T. A. M. Msagati, N. T. Tavengwa, H. J. O. Ogola, G. Ijoma, J. O. Odiyo, *Environ. Sci. Poll. Res. Int.*, **16**, No. 7, 480–488 (2019).
11. C. J. Savelli, A. Bradshaw, P. B. Embarek, C. Mateus, *Foodborne Pathogens and Disease*, **16**, No. 7, 480–488 (2019).
12. Z. Chen, T. Shen, J. Yao, W. Wang, F. Liu, X. Li, Y. He, *Molecules (Basel, Switzerland)*, **24**, No. 13, 2517 (2019).
13. J. M. R. Antoine, F. L. A. Hoo, C. N. Grant, *Toxic. Rep.*, **4**, 181–187 (2017).
14. S. Farahani, N. Eshghi, A. Abbasi, F. Karimi, E. S. Malekabad, M. Rezaei, *Toxin Rev.*, **34**, No. 2, 96–100 (2015).
15. R. Chekri, E. Le Calvez, J. Zinck, J. C. Leblanc, V. Sirot, M. Hulin, L. Noël, T. Guérin, *J. Food Comp. Anal.*, **78**, 108–120 (2019).
16. M. M. Keszycka, X. Cama-Moncunill, M. P. Casado-Gavalda, Y. Dixit, R. Cama-Moncunill, P. J. Cullen, C. Sullivan, *Trends Food Sci. Tech.*, **65**, 80–93 (2017).
17. X. Li, Y. Yang, G. Li, B. Chen, W. Hu, *Plasma Sci. Tech.*, **22**, No. 7, 122–126 (2020).
18. A. Lang, D. Engelberg, N. T. Smith, D. Trivedi, O. Horsfall, A. Banford, P. A. Martin, P. Coffey, W. R. Bower, C. Walther, M. Weiß, H. Bosco, A. Jenkins, G. T. W. Law, *J. Hazard Mater.*, **345**, 114–122 (2018).
19. R. Gaudiuso, E. Ewusi-Annan, N. Melikechi, X. Sun, Be. Liu, L. F. Campesato, T. Merghoub, *Spectrochim. Acta B: At. Spectrosc.*, **146**, 106–114 (2018).
20. S. Schröder, K. Rammelkamp, F. Hanke, I. Weber, D. S. Vogt, S. Frohmann, S. Kubitza, U. Böttger, H. W. Hübers, *J. Raman Spectrosc.*, **51**, No. 9, 1667–1681 (2020).
21. E. C. Ferreira, José A. G. Neto, Débora M. B. P. Milori, E. J. Ferreira, J. M. Anzano, *Spectrochim. Acta B: At. Spectrosc.*, **110**, 96–99 (2015).
22. R. H. El-Saeid, M. Abdelhamid, M. A. Harith, *Spectrochim. Acta B: At. Spectrosc.*, **116**, 1–7 (2016).
23. Q. Wang, G. Teng, C. Li, Y. Zhao, Z. Peng, *J. Hazard Mater.*, **369**, 423–429 (2019).
24. A. Jabbar, M. Akhtar, S. Mahmood, R. Ahmed, M. A. Baig, *Anal. Lett.*, **53**, No. 8, 1328–1341 (2020).
25. X. Cama-Moncunill, M. M. Keszycka, P. J. Cullen, C. Sullivan, M. P. Casado-Gavalda, *Food Chem.*, **309**, 125754 (2020).
26. Y. Tian, Q. Chen, Y. Lin, Y. Lu, Y. Li, H. Lin, *Spectrochim. Acta B: At. Spectrosc.*, **175**, 106027 (2021).
27. A. A. Pervin, S. Banu, B. Scott R, P. Kamaranga, T. Michael, A. Hakan, B. İ. Hakkı, *J. Sci. Food Agric.*, **101**, No. 3, 1076–1084 (2020).
28. V. C. Costa, D. V. Babos, F. W. B. Aquino, A. Virgílio, F. A. C. Amorim, E. R. Pereira-Filho, *Food Anal. Methods*, **11**, No. 7, 1886–1896 (2018).
29. H. M. Velioglu, B. Sezer, G. Bilge, S. E. Baytur, I. H. Boyac, *Meat Sci.*, **138**, 28–33 (2018).
30. B. Sezer, G. Bilge, A. Berkkan, U. Tamer, I. H. Boyaci, *Food Chem.*, **240**, 84–89 (2018).
31. Y. Liu, X. Gao, X. Jiang, H. Gao, X. Lin, Y. Zhang, Y. Zheng, *Spectrosc. Spectr. Anal.*, **40**, No. 9, 2815–2820 (2020).
32. L. Wang, T. Liu, Y. Chen, Y. Sun, Z. Xiu, *Chin. J. Biotech.*, **33**, No. 1, 68–78 (2017).